J Mater Sci: Mater Med (2010) 21:33–44
DOI 10.1007/s10856-009-3838-6

# Hybrid structure in PCL-HAp scaffold resulting from biomimetic apatite growth

**M. Lebourg · J. Suay Antón · J. L. Gomez Ribelles**

Received: 6 May 2009 / Accepted: 24 July 2009 / Published online: 29 August 2009


**Abstract** Polymer–ceramic composites are favourite candidates when aiming to replace bone tissue. We present here scaffolds made of polycaprolactone-hydroxyapatite (PCL-HAp) composites, and investigate in vitro mineralisation of the scaffolds in SBF after or without a nucleation treatment. In vitro bioactivity is enhanced by HAp incorporation as well as by nucleation treatment, as demonstrated by simulated body fluid (SBF) mineralization. Surprisingly, we obtained a hybrid interconnected organic-inorganic structure, as a result of micropore invasion by biomimetic apatite, which results in a mechanical strengthening of the material after two weeks of immersion in SBF×2. The presented scaffolds, due to their multiple qualities, are expected to be valuable supports for bone tissue engineering.

## 1 Introduction

Scaffolds are used in tissue engineering as a physical and biological support for seeding cells, and transplanting them into an organism. In the field of bone tissue engineering, polymer matrix/ceramic load composites have been drawn to attention as promising materials for tissue scaffolding, for they may combine both the advantages of polymer materials and ceramics. Synthetic biomedical polymers such as polycaprolactone (PCL), or polylactide (PLA), polyglycolide (PGA), and their copolymers (PLGA) are easy to process in porous forms, and their ductile nature permits a good fit into the defects; their major drawback is that they do not show any intrinsic bioactivity, or in other words, they do not induce any positive regenerative response from bone cells when implanted. On the other hand, some ceramics, among which calcium phosphates (BCP, TCP), Bioglass and hydroxyapatite (the mineral phase of bone), have been shown to have positive effects on bone formation and cell fate in vivo and in vitro. Unfortunately, due to their nature, they are brittle, and can hardly be processed into porous structures as interconnected needed for cell spreading and colonisation. For better biological results and user-friendliness (possibility for the surgeon to fit the implant into the defect shape), the use of composites has thus been considered. Various studies have assessed the effect on cell response of the incorporation of an inorganic phase (calcium phosphates or Bioglass®) into biocompatible polymers like PCL, PLA or PLGA. All considered studies have shown improved biocompatibility and higher expression of osteogenic markers when HAp [1–3] or Bioglass is incorporated to the polymers. This behaviour may be partially explained by an improved adsorption of binding extracellular matrix (ECM) proteins—such as fibronectin or vibronectin—to composites as compared to neat polymers [4]. Besides, a biomimetic technique consisting of the deposition of bone-like apatite onto polymeric scaffolds in simulated body fluid has been developed, based on the works of Kokubo and co-workers [5, 6]. His group first described the composition of a solution called simulated body fluid (further called SBF), which is able to reproduce in vitro changes

M. Lebourg (✉) · J. S. Antón · J. L. G. Ribelles
CIBER en Bioingeniería, Biomateriales y Nanomedicina, Valencia, Spain
e-mail: myle1@doctor.upv.es

J. S. Antón · J. L. G. Ribelles
Center for Biomaterials and Tissue Engineering, Universidad Politécnica de Valencia, 46022 Valencia, Spain

J. S. Antón · J. L. G. Ribelles
Regenerative Medicine Unit, Centro de Investigación Príncipe Felipe, Autopista del Saler 16, 46013 Valencia, Spain

that normally occur physiologically when a bioactive material is implanted in the body prior to bone bonding, namely the deposition of an apatite layer on the surface of the material. This simulated body fluid has nearly the same electrolyte concentration as human blood plasma [5] and can therefore be used to assess easily in vitro the bioactivity of a material, where the speed of apatite deposition has been related to the in vivo bone bonding ability [6]. The mechanisms for deposition of biomimetic apatite in SBF have been described for various materials: it is generally argued that the deposition is related with negative surface potential of the materials. Moieties that are likely to be deprotonated at physiological pH, such as maybe –COOH, –TiOH, –OH, –SiOH, $–PO_4H_2$, and thus induce negative surface charge, are effective for nucleating biomimetic apatite [6–8]. The mechanism has been studied in detail by Kokubo et al. on hydroxyapatite, and is likely to be similar on other bioactive surfaces: due to the negative surface potential calcium cations are attracted. Calcium-rich amorphous calcium phosphate is then deposited, until surface potential is inversed; then phosphate-rich amorphous calcium phosphate is deposited; this amorphous inorganic layer finally crystallizes into apatite [9]. The so-formed apatite is known to be carbonated, moderately crystalline, and to contain substitution atoms like Mg and Na; it is thus more similar to bone apatite than synthetic (highly pure and crystalline) ones, and generally described as biomimetic or bonelike apatite [10, 11]. Based on the assumption that biomimetic apatite-coated materials would show a better cellular response than uncoated ones, SBF-coating or synthesis of biomimetic apatite-polymer [12] hybrid materials has been approached as a strategy per se, not for assessing in vitro bioactivity, but with the aim of obtaining better biological properties; the inclusion of proteins during coating has been considered as well [13, 14], and also the synthesis of apatite by a chemical way using SBF as a reaction medium was carried out [15, 16].

Various posterior works have focussed their attention on the formulation of improved SBF, multiplying SBF concentration to accelerate the apatite formation [17, 18], modifying the carbonate concentration [19–21] or the pH of SBF [22]; all these factors have been seen to have a decisive influence on the properties of the apatite formed (crystallinity, Ca/P ratio, A or B-type substitution, crystal growth orientation, etc.) [19–21].

In spite of the fact that hydroxyapatite particle incorporation has been described as beneficial for cell response, the expected positive effect of biomimetic coating on cells is controversial. Some authors claim to obtain better proliferation of osteoblasts or osteoblast precursor cells, osteogenic markers expression (alkaline phosphatase and osteocalcin production), or osteoblast-like morphology [1, 12, 13, 17], when materials are coated with or contain biomimetic apatite. On the other hand, other authors obtain worse results with coated materials [10, 23] or even state that mesenchymal stem cell differentiation may be inhibited by bone-like mineral film [24]. These discrepancies will be later discussed but, as clearly appears in the study of Chou et al. [22], cells react to slight variations in chemistry and morphology of apatite, giving rise to contradictory results if the precise composition, morphology and above all solubility of the formed apatite is not assessed.

In this work, we synthesized interconnected porous scaffolds of poly(ε-caprolactone) and poly(ε-caprolactone)-hydroxyapatite composites using a mixed process of porogen leaching and phase inversion. Polycaprolactone has been used in various studies, giving good results for bone tissue engineering, and better results when mixed with an inorganic phase like hydroxyapatite. We then used a treatment for promoting apatite bonding ability [25] and subjected the scaffolds to SBF immersion; untreated samples were used as well in order to compare the results obtained. The scaffolds were then characterized by means of microscopy, elemental analysis, thermogravimetry, and the effect of HAp coating on mechanical properties was evaluated with compression tests. The particularity of the materials obtained here is a hybrid structure resulting from interpenetration of the mineral phase with the microstructure of the scaffolds during the coating process which, to our knowledge, has not been described before.

## 2 Materials and methods

### 2.1 Preparation of the scaffolds

PCL Mw = 43000–50000 was furnished by Polysciences. HAp particles of mean size 90 nm were a courtesy from the Centre for Biomaterials of la Habana, Cuba. 1,4-Dioxane and ethanol of purity 98% were bought from Scharlab and used as received.

The sheets of neat PCL used for surface characterization measurements were prepared by melting PCL pellets between two glass plates at 90°C for 20 min and subsequent cooling in air.

Scaffolds were prepared by a mixed particle leaching/freeze extraction process. Low molecular weight polyethylmethacrylate (PEMA) beads (from Lucite International) with mean diameter 200 μm were used as a porogen. Freeze extraction is a modification of freeze drying as proposed by Wang and co-workers [26], which saves time by dissolving the solidified solvent instead of sublimating it. In our case, dioxane was used as a solvent, and it was dissolved in the freezer at −20°C in ethanol.

First hydroxyapatite nanoparticles were dispersed in dioxane by ultrasonic exposure. Then polycaprolactone was added and dissolved under constant stirring. The ratio PCL/dioxane was 17.6% by weight in all the scaffolds. The nanoparticle content in the composites was 2.5, 7.5 or 15% by weight with respect to PCL, nanocomposite samples will be referred to as PCL2.5HAp, PCL7.5HAp, PCL15HAp, respectively. The solution was mixed with PEMA beads in a weight ratio 4/5 and immediately frozen in liquid nitrogen. Solvent extraction was performed in cold ethanol at −20°C as described in [26]; ethanol was changed three times. Subsequently particle leaching was performed in ethanol at 40°C. The first series of samples obtained in this way showed a systematic and proportional shift of the HAp nanoparticles content measured by thermogravimetry compared to the expected content. We related it to the leaching of a part of the particles during solvent/porogen extraction, also supported by the observation of some white coloration of the ethanol during extraction. In consequence, we added the adequate excess of nanoparticles to reach the desired content.

## 2.2 Biomimetic HAp deposition

A series of nanocomposite scaffolds was treated with a 1 M sodium hydroxide solution for 1 day at room temperature, and then submitted to alternate $Ca/PO_4$ solutions dipping, as a way to generate calcium phosphate nuclei and enhance apatite formation ability, as described in [25]. Shortly, after basic attack of sodium hydroxide, the scaffolds were rinsed with ultrapure Millipore water, plunged for 10 s in 0.2 M $CaCl_2$ aqueous solution, rinsed with ultrapure Millipore water for 1 s, plunged for 10 s in 0.2 M $K_2HPO_4$ aqueous solution, rinsed with ultrapure Millipore water for 1 s. $CaCl_2$ and $K_2HPO_4$ aqueous solutions were prepared with ultrapure Millipore water. The whole dipping cycle was repeated three times. The samples that were subjected to this treatment are thereafter designated as treated samples.

Control scaffolds were immersed directly in SBF without nucleating treatment to verify the influence of the treatment on apatite-nucleating ability. Subsequently the scaffolds were immersed in simulated body fluid, SBF, with the following molar concentrations: $Na^+$ 142.0; $K^+$ 5.0; $Mg^{2+}$ 1.5; $Ca^{2+}$ 2.5; $Cl^-$ 148.8; $HCO_3^-$ 4.2; $HPO_4^{2-}$ 1.0; $SO_4^{2-}$ 0.5 buffered at pH 7.4 with Trishydroxymethylaminomethane (0.5 M) and hydrochloric acid (1 M), prepared as described in [6]. The SBF was changed weekly in order to replace the precipitated ionic species and ensure a nearly constant ionic activity.

A second group of samples used for mechanical testing was treated with the mentioned treatment and immersed in SBF×2 (twice the mentioned ionic concentrations) for two weeks to accelerate the mineralization process as described by Kim et al. [17]. The SBF was changed weekly as in the first series. The quantification of the deposited apatite in these scaffolds was carried out by weighing them, yet the process had to be non-destructive to permit further use of the scaffolds for mechanical testing.

During all the immersion procedures, great care was paid to the correct wetting of the scaffold since PCL is very hydrophobic and hard to wet with aqueous solutions; moreover, the synthesized scaffolds show high specific surface area; in order to ensure the correct wetting of all internal surfaces of the scaffolds after immersion in SBF, they were submitted to depressurization/pressurization cycles in ultrasonic bath until they stopped bubbling in vacuum.

## 2.3 Porosity measurement

Porosity was measured by gravimetric means. The samples were weighed dry, filled with ethanol under vacuum, and subsequently weighed again. Porosity was calculated as the quotient of the volume of pores (see below) and the total volume of the scaffold.

The volume of pores, $V_{pore}$, was deduced from the weight difference between dry ($m_{dry}$) and wet ($m_{wet}$) sample, according to Eq. 1 assuming that the amount of ethanol absorbed by the PCL phase is negligible during the sort time of the experiment. Thus, the volume of pores equals the volume occupied by the absorbed ethanol.

$$V_{pore} = \frac{m_{wet} - m_{dry}}{d_{ethanol}} \quad (1)$$

where $d_{ethanol}$ is the density of ethanol.

The volume of polycaprolactone was calculated from the dry weight of the scaffold assuming as density of PCL 1.135 g $cm^{-3}$, which corresponds to the average crystallinity measured by DSC, close to 62%. Density was calculated on the basis of amorphous phase and crystalline phase densities of respectively 1.021 and 1.2 g $cm^{-3}$ [27].

## 2.4 SEM observation and elemental analysis

Samples were fractured in liquid nitrogen, mounted on a copper stub, gold sputtered and observed with a JEOL JSM6300 scanning electron microscope with an acceleration tension of 10 kV. Energy dispersive X-ray analysis (EDX) was performed in order to analyze the quantitative composition of the deposited mineral: calibration of the detector was realized with copper standards.

## 2.5 Fourier transform infrared analysis

Chemical surface changes with nucleation treatment were studied using an FTIR Thermo Nicolet Nexus apparatus in

ATR mode. Surfaces of untreated, sodium hydroxide treated, and apatite covered samples were measured.

### 2.6 Contact angle measurement

Contact angle measurement with water was performed by sessile drop method, using a Dataphysics OCA20 device equipped with a Nikon Camera; contact angles were calculated using image analysis software. Results were averaged from a set of at least five drops.

### 2.7 TGA measurements

Thermogravimetric analysis (Thermogravimetric analyzer SDTQ600 from TA Instruments) was used in order to determine the quantity of HAp nanoparticles and biomimetic deposited HAp in the samples. The samples were subjected to a temperature ramp from room temperature until 700°C, at 20°C/min under nitrogen flow (50 ml/min).

### 2.8 Mechanical analysis

In order to determine the influence of bonelike apatite formation on the mechanical properties of the PCL scaffolds, compression tests were conducted before and after apatite treatment. The samples were cut into pieces of $5 \times 5 \times 3$ mm approximately, and compressed in a Microtest standard compression machine with a 15 N load cell. Mechanical properties were evaluated following the guidelines of ASTM norm D1621-04a "Compression of rigid cellular plastics"; the presented results are mean values of at least 5 measurements. Statistical analysis was used to compare results of diverse scaffold types: a *t*-test was used and differences were considered significant for $P < 0.05$.

## 3 Results

### 3.1 Structure of the scaffolds

As can be seen in Fig. 1, scaffolds show double pore structure due to the production process. Porogen leaching leads to an interconnected macroporous structure with pores of around 200–300 μm connected by large necks, whereas solvent crystallization and subsequent dissolution leads to microporosity with micrometric channelled structure. The porosity of the scaffolds reached 85 ± 1.7%; the porosity of the pure PCL scaffold was slightly higher than the porosity of composite scaffolds (PCL: 86.4 ± 2.4%; PCL2.5HAp: 86.0 ± 2.1%; PCL7.5HAp: 85.22 ± 0.1%; PCL15HAp: 83.51 ± 0.7%), but as can be seen in SEM pictures, the overall structure was not affected by HAp nanoparticles incorporation. As can be seen in the SEM micrographs taken at higher magnification (Fig. 2), many HAp nanoparticles appear on the inner surfaces of the

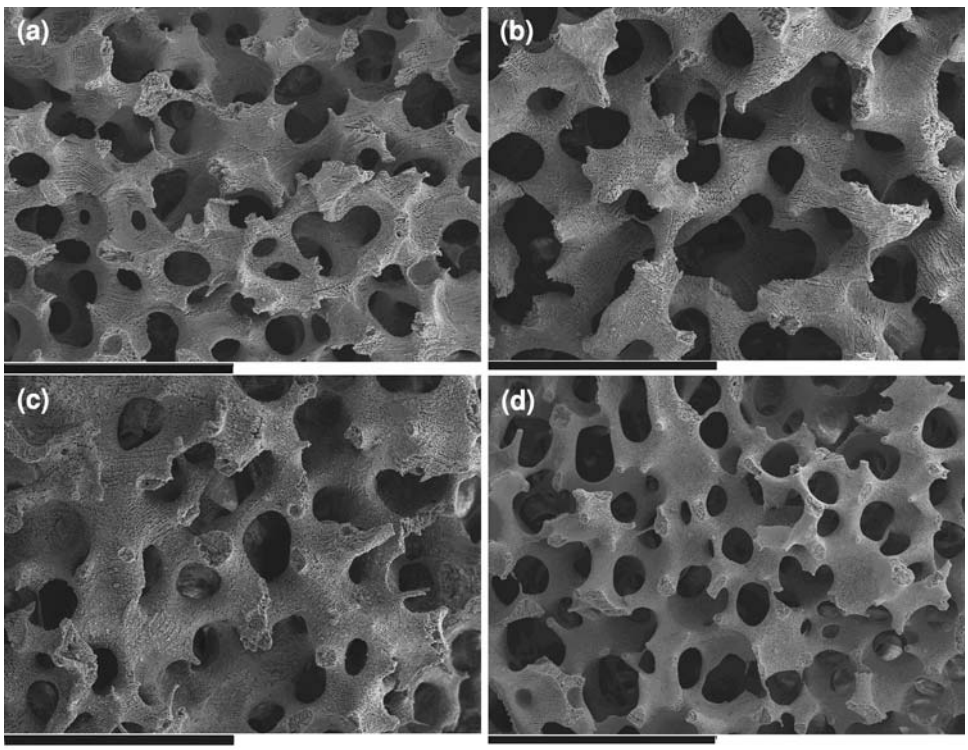


**Fig. 1** Composite scaffolds synthesized by mixed freeze-extraction process: pure PCL (**a**); PCL with 2.5% HAp (**b**); PCL with 7.5% HAp (**c**); PCL with 15% HAp (**d**) (dimension bar 600 μm)

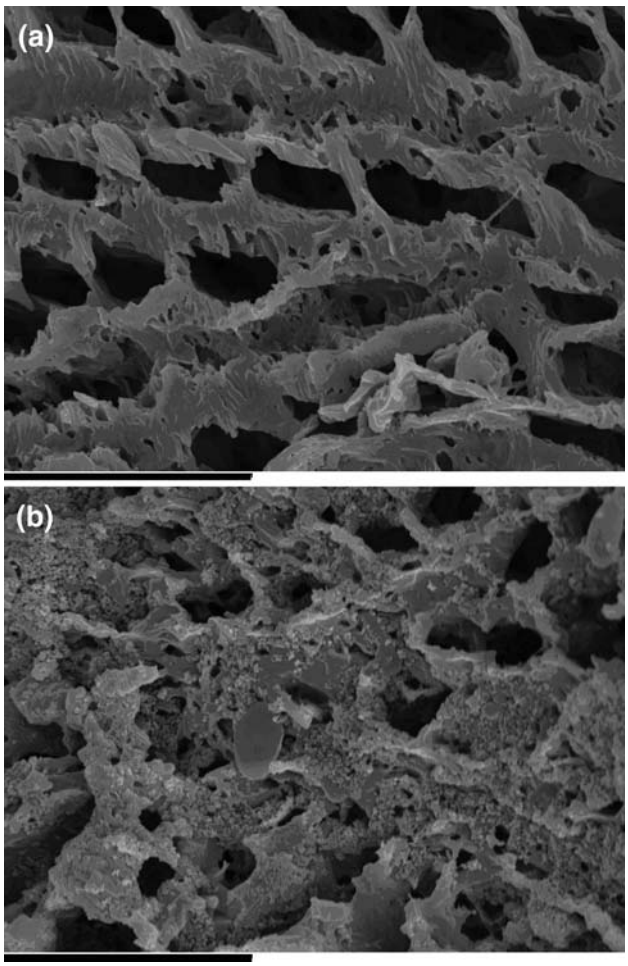


**Fig. 2** A comparison of the surface of a pure PCL scaffold (**a**) and a scaffold with 7.5% HAp particles (**b**) ×5000 (dimension bar 10 μm)

scaffolds, which is likely to be due to their expelling by the crystallization front of PCL during tempering (DSC measurements show that PCL scaffolds are highly crystalline after freeze extraction process, data not shown) [28].

On the other hand, the inclusion of HAp particles seems to have a nucleating effect in the crystallization of dioxane when freezing the PCL/HAp/dioxane solution since the microstructure observed for scaffold with 15% HAp is much finer than that of neat PCL, which means that smaller dioxane crystals were formed on freezing.

### 3.2 The composition of the nanocomposite scaffolds

TGA residue analysis provides information about the actual composition of the composites. In a first set of samples loaded with HAp but before any treatment, a systematic deviation of 30% from the nominal concentration was observed. It was related to the leaching of some HAp particles during the elimination of dioxane and porogen. Consequently the following sets of samples were synthesized with a proportional excess of HAp particles in order to obtain the desired concentrations after leaching out the porogen.

### 3.3 Surface analysis of bulk samples

In order to deposit a layer of biomimetic hydroxyapatite on the internal surface of the porous structure of the scaffold, it was subjected to different treatments to facilitate the nucleation of the HAp crystals on the surface. Characterizing the effect of such treatments on the bended surface of the scaffold trabeculae is not easy, thus, flat sheets of neat PCL were subjected to the same treatments to characterize the change induced in the surface properties.

Wettability was greatly enhanced by surface treatment with sodium hydroxide, as can be seen in Fig. 3 (contact angle with water changed from 72.5 ± 0.5° to 37 ± 1° upon etching with sodium hydroxide). When the surface was coated with a layer of biomimetic apatite after three weeks immersion in SBF there was a light wettability improvement that was nevertheless not decisive. An average value of the contact angle of 31.4 ± 3.4° was measured but with large scattering in the results probably due to the heterogeneity of the mineral layer. (This means a change of only 6° to 31.4 ± 3.4° with respect to the sample treated with sodium hydroxide.)

Analysis of the sample surface with FTIR after etching with sodium hydroxide treatment showed an increased proportion of C–O bonds with respect to ester bonds (Fig. 4a) [25] as well. The effect increased with longer treatment times. Detail of the 1600–1500 $cm^{-1}$ zone (Fig. 4b) shows the apparition of a resonance band due to coupling of COO vibration of the carboxylic groups created by scission of ester groups through attack of the hydroxide; these moieties are likely to be deprotonated and substituted with Na ions or hydrated, allowing strong coupling of both oxygen stretching.

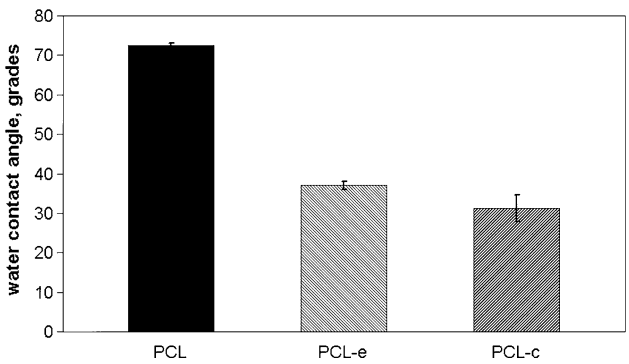


**Fig. 3** The variation of PCL films contact angle with water after surface treatment: etched with NaOH (PCL-e) and covered with biomimetic apatite (PCL-c)

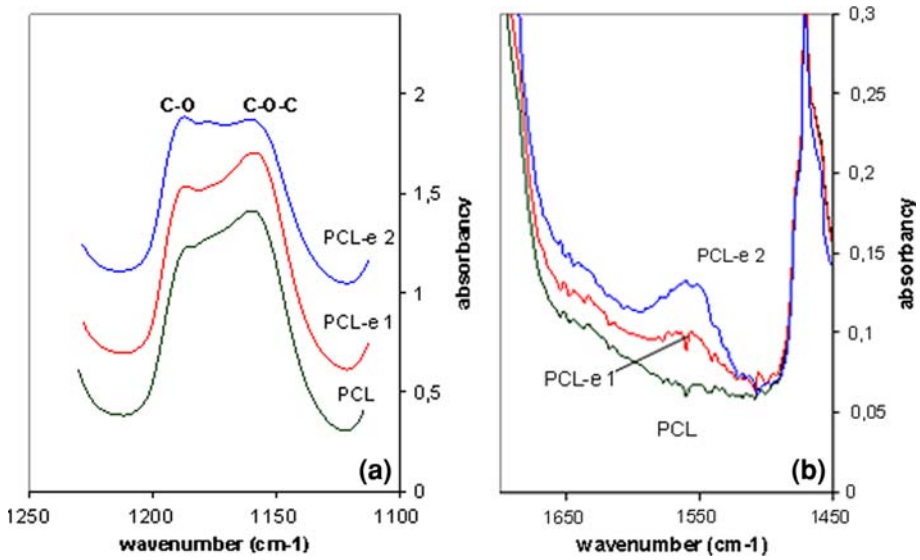


**Fig. 4** Changes in the spectra of PCL solvent cast films after etching for 1 day (PCL-e1) and 2 days (PCL-e2) with molar sodium hydroxide. Change of C–O/C–O-C ratio (**a**). COO resonance band in the 1450–1650 region (**b**)

Results of FTIR can explain the increase in wettability with water observed by sessile drop measurement by the increase of polar groups with respect to aliphatic backbone that happens due to basic chain scission. At the same time, it has been observed that etched porous samples and treated samples, when subjected to TGA, lose more bound water at low temperatures: in the same way, a wide peak due to intermolecular hydrogen bonds with bound water is observed in FTIR spectra at 3000–3500 $cm^{-1}$ on these samples (data not shown), confirming the hydrophilization of the surface.

After coating with the apatite layer (Fig. 5), the characteristic peaks for PCL disappear, and phosphate associated peaks are seen: at 964 $cm^{-1}$, the $v_1$ mode of phosphate, and in the range between 970 and 1135 $cm^{-1}$, the $v_3$ stretching mode, as well as weak peaks associated with $CO_3^{2-}$ at 1460, 1420 and 875 $cm^{-1}$ (characteristic for B-type substitution, where $CO_3^{2-}$ substitutes phosphate moieties). Nonetheless, the strong peaks at 1695–1735 $cm^{-1}$ associated with carbonyl stretching, or the peaks at 2800–3000 $cm^{-1}$, typical for $CH_2$ symmetrical and asymmetrical stretching of the PCL backbone, do not appear; this means that the coating is quite thick and spread over the whole surface of the sample, reflecting all the infrared beam. The spectrum thus shows nearly no polymer-associated frequencies.

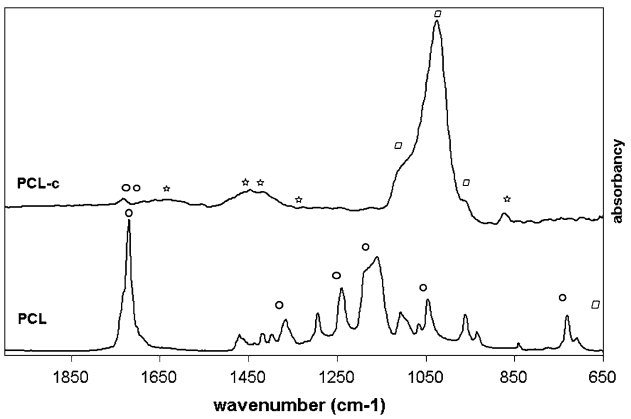


**Fig. 5** FTIR-ATR spectrum of untreated (PCL) and apatite-covered PCL film (PCL-c): phosphate group (◇), carbonate group (☆) and groups from polymer moieties (○)

### 3.4 Deposition of biomimetic apatite on PCL scaffolds

Apatite was successfully deposited on PCL after nucleation treatment by immersion in alternate $Ca/PO_4$ solutions and as can be seen on the micrographs in Fig. 6. The EDX analysis of the deposited apatite layer shows peaks which are characteristic of the presence of impurities such as potassium, chlorine and magnesium (Fig. 6b), which is common for biomimetic apatite. Nevertheless, untreated pure PCL did not support the growth of an apatite layer as can be seen for treated samples. Some mineral was deposited but EDX reveals that unspecific precipitation of various salts occurred and the characteristic cauliflowers shape of apatite crystals was scarcely observed, even after 2 weeks of SBF immersion as shown in Fig. 6a and in Fig. 7 at higher magnification. In the case of the composites the deposition of mineral in the untreated samples increases with respect to pure PCL scaffolds, but still the composition is not always that expected for hydroxyapatite even if the morphology observed in the SEM microphotographs resembles that of biological apatite (Fig. 7). The nucleating effect of synthetic HAp nanoparticles seems to increase with the quantity present on the surface, as PCL15HAp showed the most apatite formation with a dense layer of cauliflower shaped crystals covering all the

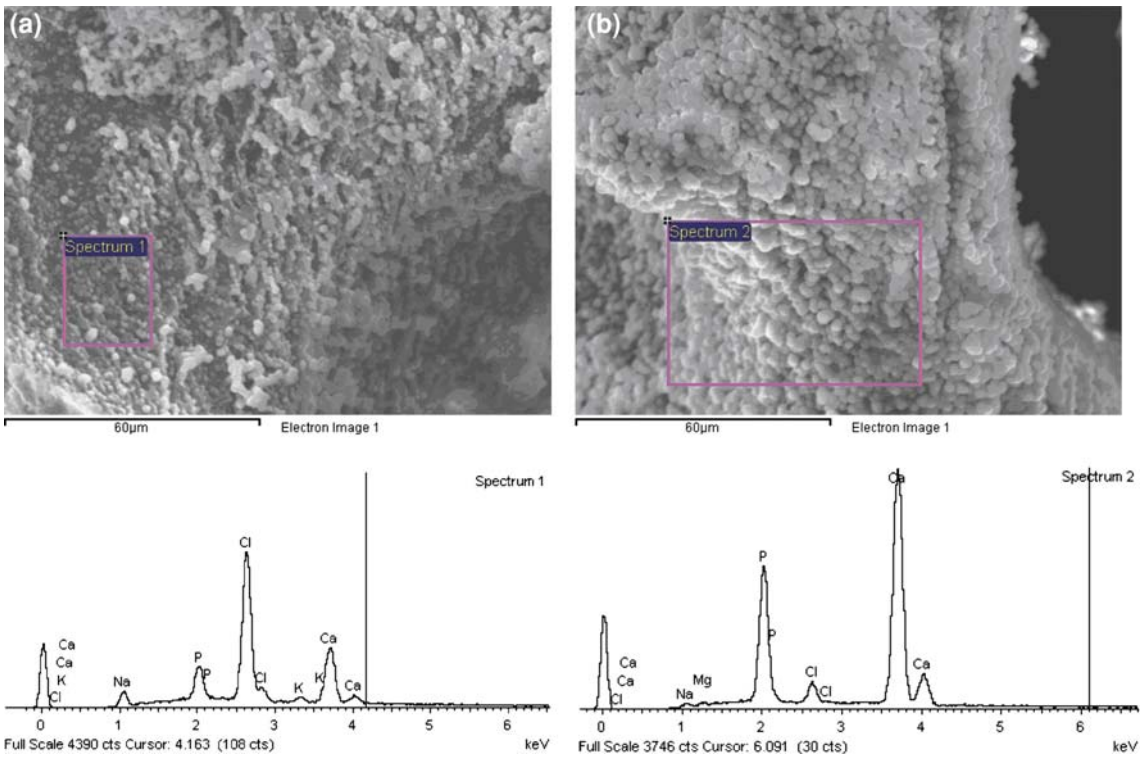


**Fig. 6** Spectra for undifferentiated mineral deposition (chlorine ions (**a**)) on an untreated sample and for calcium phosphate, apatite precursor deposition on a treated sample (**b**) (PCL neat samples, 3 weeks in SBF)

structure (Fig. 7c). Quantitative results of element proportions in the deposited mineral layer are listed in Table 1. The ratios of Ca/P and Cl/P are represented as an indicator for the specificity of the deposition. A bone-like hydroxyapatite layer should present a Ca/P ratio close to 1.65 which is the value reported for bone. High chlorine ion content should indicate undifferentiated precipitation and is not indicative for bone bonding ability.

The total amount of mineral deposited in the nucleated scaffolds was measured with TGA as a function of the immersion time in SBF (Fig. 8). The results are shown for pure PCL where the trend is really representative, whereas uncertainty in HAp previous content of composites samples makes interpretation harder. As can be seen, the nucleation treatment is really effective for the induction of apatite deposition; when a latency time is observed for untreated PCL, the treatment immediately nucleates the mineral phase on the surfaces of pure PCL scaffolds, which is likely to be due to dissolution, local concentration variation of SBF and reprecipitation by local increase of the supersaturation. Nevertheless, it is important to note that these measurements have to be interpreted with care since, as we commented above, unspecific mineralization may occur concurrently or simultaneously with apatite deposition; at the same time, carbonate ions may be—at least partially—thermally degraded during thermal scan.

### 3.5 Hybrid structure

Amazingly, we discovered that treated samples that had been coated for two or three weeks in SBF, showed after calcination at 700°C in nitrogen atmosphere in the TGA (Fig. 10), a residue that conserved the initial shape of the scaffold (also when not showing much mechanical resistance and crumbling when held with a clamp). Figure 10 shows a micrograph of the TGA residue of a 15HAp treated scaffold after 3 weeks in SBF. The structure of the residue is the same as that of the scaffold. So the apatite actually precipitates within the micropores of the structure, as can be seen in Fig. 9, and the scaffold turns into an interpenetrated network of inorganic coating and polymeric matrix.

### 3.6 Mechanical testing

The results of the compression tests for the uncoated and coated samples are presented in Fig. 11. Between untreated samples, the incorporation of HAp nanoparticles is seen to have a strengthening effect on the elastic modulus as well as on the yield stress of the scaffolds. The series of samples used to study the strengthening effect of the biomimetic HAp coating was subjected to a nucleation treatment and then immersion in SBF until a weight fraction of apatite

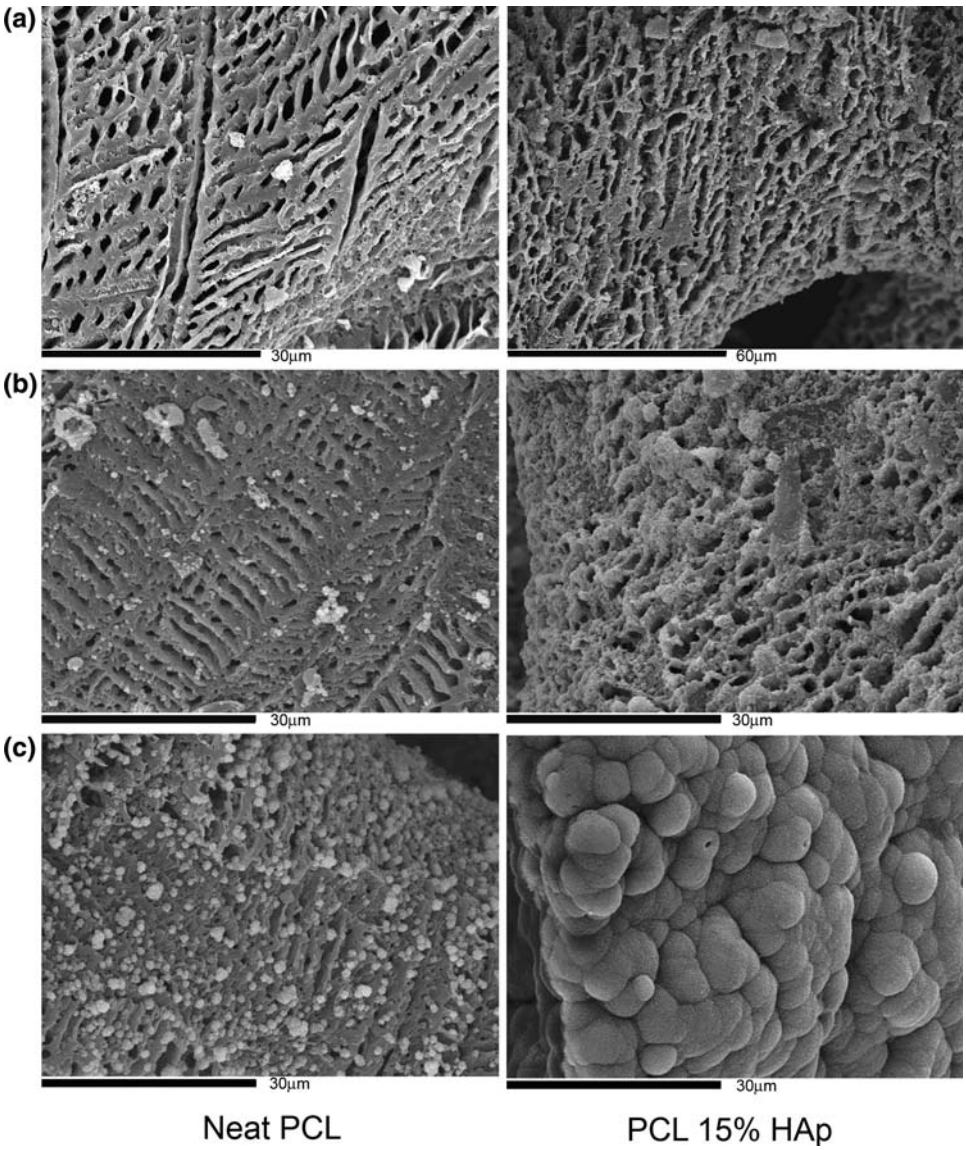


**Fig. 7** The evolution of mineral layer deposition after SBF immersion of untreated samples over one (**a**), two (**b**) or three (**c**) weeks for neat PCL (*left*) and PCL15HAp (*right*) (bar size 30 μm excepted PCL15HAp (**a**), 60 μm)

**Table 1** Atomic Ca/P and Cl/P ratios measured from EDX element analysis

| | Ratio Ca/P | Ratio Cl/P |
|---|---|---|
| *Control group (without treatment)* | | |
| Pure PCL | 2.3 | 3.4 |
| 2.5 HAp | 3.4 | 3.1 |
| 7.5 HAp | 2.7 | 3.5 |
| 15 HAp | 3.4 | 0.5 |
| *Nucleation treatment* | | |
| Pure PCL | 2.3 | 0.1 |
| 2.5 HAp | 1.3 | 0.5 |
| 7.5 HAp | 1.6 | 0.2 |
| 15 HAp | 1.6 | 0.4 |

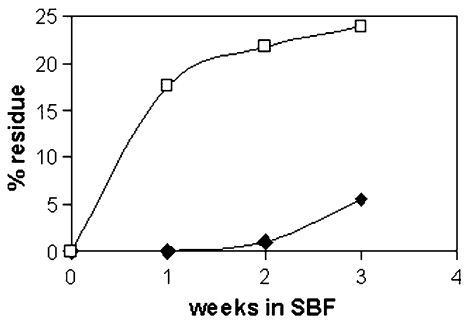


**Fig. 8** Mineral deposition, in weight percent after immersion in SBF for different times, calculated by the residual weight after calcinations at 700°C, for pure PCL without treatment (◆), and with nucleation treatment (□)

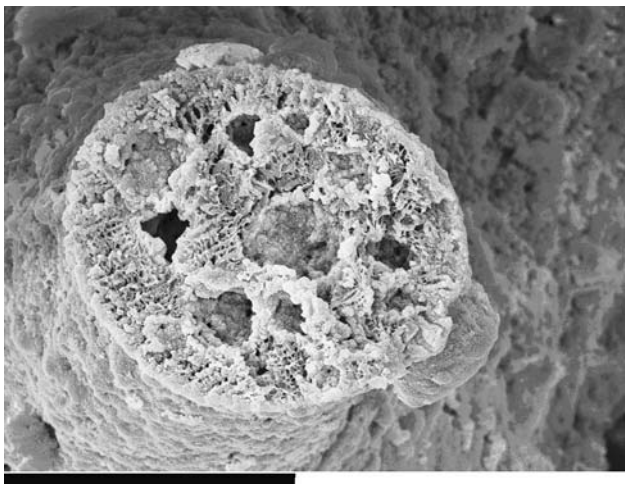

**Fig. 9** Penetration of the mineral phase into the microstructure of the scaffold (7.5HAp treated, 3 weeks in SBF) (bar size 40 μm)

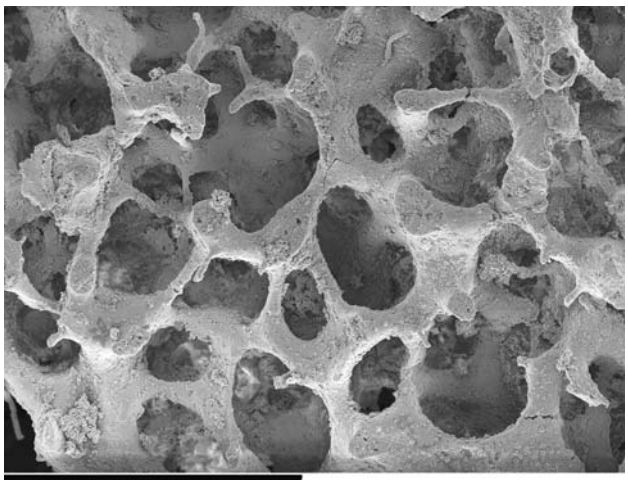

**Fig. 10** Micrograph of the pyrolysis residue of a PCL 15HAp composite treated with nucleation treatment and covered with biomimetic apatite for three weeks in SBF (bar size 400 μm)

with respect to PCL weight of around 30% was attained in all samples in order to obtain comparable results. In the case of the pure PCL scaffold and also in the composite scaffold containing 15% HAp nanoparticles both the elastic modulus and yield stress are seen to be significantly higher in the scaffolds coated with biomimetic HAp than in the uncoated ones, whereas the difference is not significant for PCL 7.5%HAp and PCL 2.5%HAp samples.

## 4 Discussion

### 4.1 Hydroxyapatite coating formation

Much has been written about apatite layer formation on materials in simulated body fluid. However, in many

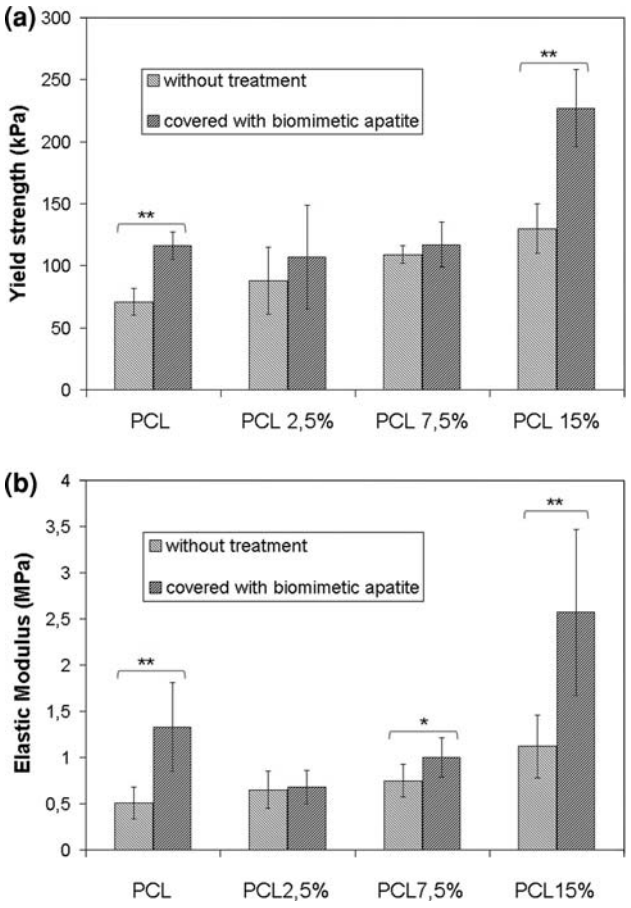


**Fig. 11** Evolution of yield stress (**a**) and Young modulus (**b**) after apatite deposition on scaffolds (* $P < 0.1$, ** $P < 0.05$)

papers, there is no qualitative assessment of basic properties of the so-called apatite, such as atomic composition, Ca/P ratio, crystal morphology and crystallinity. This aspect is fundamental when related to biological properties, since cells react very differently depending, for example, on coating crystallinity: amorphous calcium phosphate has been shown to provoke cytotoxicity in vitro and in vivo, likely because of high concentrations of both calcium and phosphates (Adams et al. showed that these ions provoke apoptosis of bone cells in a synergistic way [29]). The dissolution of other phases possibly present in the coating, as for example CaO, has been shown to provoke a basification of cell culture medium in vitro, which is associated with increased cell death rate [30]. Here, the coatings described have been characterized with SEM and elemental analysis, revealing that all the expected elements are contained and indicating that calcium phosphates are being deposited. Nonetheless, in some cases, undifferentiated precipitation of other electrolytes occurs, for reasons that are not really understood. It has been shown that a positive polarization of an apatite surface favours calcium chloride precipitation at the expense of apatite deposition during

immersion in SBF [31]. In our groups, results of PMMA scaffolds led to calcium chloride deposition (unpublished results), maybe due to such surface potential effects. In some cases, it may be that incomplete porogen leaching favoured calcium chloride deposition in some scaffolds. Here we are dealing with very porous materials that have a huge specific surface owing to their double pore structure, which facilitates the local variation of SBF concentration an thus the precipitation of all kinds of salts (the scaffolds are coated much faster than the sheets of PCL); this physical property was described as a drawback in the critical article of Bohner and Lemaitre on testing bioactivity with SBF solution [32]. The nucleation of the mineral phase is highly enhanced by the presence of hydroxyapatite particles, as can be seen on the micrographs from Fig. 7. Whereas pure PCL shows scarce nuclei with typical pre-apatite shape [22], PCL15HAp shows dense coating with cauliflower structure as usually described for apatite; this is the confirmation that hydroxyapatite introduction into the PCL matrix causes an improved biocompatibility of the scaffold.

Besides, the effect of the nucleation treatment is positive regarding the amount of apatite deposited and the speed of deposition, chloride precipitation, as well as regarding the Ca/P ratios of the mineral layer. A ratio close to 2.5, which is the ratio of calcium to phosphate present in SBF, is more indicative for deposition of amorphous calcium phosphate than for apatite, with the associated problems if considering a use of the covered scaffolds with cells due to the cytotoxicity of amorphous calcium phosphate (a need for apatite crystallization before use).

From the FTIR measurements it can be seen that the apatite deposited is carbonated, with a B-substitution type (location of the associated peaks at 1460, 1420 and 875 $cm^{-1}$) [33], as is usually observed when a SBF with a carbonate content lower than 20 mM is used [19]) when carbonate substitutes phosphate. The carbonate substitution may be scarce because we used traditional SBF which possesses a low amount of carbonate (4.2 mM when sanguine plasma contains 27 mM) but because of a low signal/noise ratio, the 600 $cm^{-1}$ zone could not be measured accurately and quantification of $CO_3$ substitution was not possible. Crystal morphology on treated samples showed the typical cauliflower structure, with plate-like crystals organized as spherulites.

### 4.2 Interpenetrated hybrid structure and mechanical strengthening

Resulting from biomimetic apatite growth in the scaffold, an interpenetrated hybrid structure with two co-continuous phases was generated by long time-treatments, as is apparent from Figs. 9 and 10. Figure 10 shows that a high interpenetration is reached since the physical macrostructure remains when burning out the organic part of the scaffold. This was observed with samples that were mineralized for three weeks. We then designed another experiment for assessing the mechanical strengthening that can be obtained by the apatite layer deposition. As explained in Sect. 3, strengthening was effective in half of the cases considered at a statistically significant level. Explanations on why it is not effective in all cases can be sought in various directions: the interpenetration degree is the first to be considered, since although the mineralization percentage was similar in all samples, it is possible that in some cases (namely the case of PCL2.5HAp and PCL 7.5HAp), the mineralization did not result in a totally interconnected layer throughout the scaffold, thus limiting the extent of mechanical strengthening. Other possible factors are a different affectation of the polymer due to hydrolytic attack with sodium hydroxide that may weaken the polymer structure and act as a counter-effect on mechanical strengthening. Albeit we do not believe that scaffolds should be used as implants with this degree of mineralization, as according to the results by Chim et al. [23] in vivo results may be compromised by a flaking of the mineral layer under physiological stresses. Moreover, the evoked problems affecting precise layer composition and solubility should be solved in order to promote a better cell response. Nevertheless, these results are interesting since in vivo mineralization should be able to produce the same type of structure through secretion of extra-cellular matrix proteins and mineralization of this matrix, thus permitting a strengthening of the construct and a good interaction between the colonising tissue and the scaffold. As a matter of fact, a high specific surface due to mesopores has been described as a key physical factor for promoting osteoinduction [34]. De Groot and co-workers associated better osteoinductive behaviour of microporous ceramics to enhanced specific surface, that leads to enhanced reactivity in terms of dissolution and reprecipitation of biological apatite (with the possibility of co-precipitating relevant endogenous proteins which in turn initiate the differentiation of multipotent cells into the osteogenic linage [35]).

## 5 Conclusions

We were able to synthesize materials with highly interconnected macroporosity much alike to the trabeculae of spongy bone, with suitable pore size for trabeculae formation and vascularization; once treated, these materials show rapid apatite formation in SBF (clue for bone bonding), and they possess a high specific surface that is thought to enhance surface reactivity. These materials enjoy the

well-known biocompatible and bioactive character of PCL-HAp biomaterials; they may be able to rapidly strengthen when implanted due to interpenetration with extracellular matrix and mineralisation, as demonstrated by mechanical testing after in vitro biomineralisation. These are many clues which lead us to believe that these composite scaffolds should be a promising basis for bone tissue engineering.

**Acknowledgements** The support of the Spanish Ministry of Science through projects no. MAT2007-66759-C03-01 and MAT2007-66759-C03-02 (including the FEDER financial support), and Consellería Valenciana de Sanidad through project AP-111/08 is acknowledged. The authors acknowledge Dr. Mayelin Guerra for kindly providing them with hydroxyapatite nanoparticles for this study. SEM was performed under the technical guide of the Microscopy Service at the Universidad Politécnica de Valencia.

## References

1. Ciapetti G, Ambrosio L, Savarino L, Granchi D, Cenni E, Baldini N, et al. Osteoblast growth and function in porous poly ε-caprolactone matrices for bone repair: a preliminary study. Biomaterials. 2003;24:3815–24.
2. Hasegawa S, Neo M, Tamura J, Fujibayashi S, Takemoto M, Shikinami Y, et al. In vivo evaluation of a porous hydroxyapatite/poly-DL-lactide composite for bone tissue engineering. J Biomed Mater Res A. 2007;81A:930–8.
3. Shor L, Güçeri S, Wen X, Gandhi M, Sun W. Fabrication of three-dimensional polycaprolactone/hydroxyapatite tissue scaffolds and osteoblast-scaffold interactions in vitro. Biomaterials. 2007;28:5291–7.
4. Woo KM, Seo J, Zhang R, Ma PX. Suppression of apoptosis by enhanced protein adsorption on polymer/hydroxyapatite composite scaffolds. Biomaterials. 2007;28:2622–30.
5. Kokubo HK T, Sakka S, Kitsugi T, Yamamuro T. Solutions able to reproduce in vivo surface-structure changes in bioactive glass–ceramic A-W. J Biomed Mat Res. 1990;24:721–34.
6. Kokubo T, Takadama H. How useful is SBF in predicting in vivo bone bioactivity? Biomaterials. 2006;27:2907–15.
7. Oliveira AL, Mano JF, Reis RL. Nature-inspired calcium phosphate coatings: present status and novel advances in the science of mimicry. Curr Opin Solid State Mater Sci. 2003;7:309–18.
8. Kawashita M, Nakao M, Minoda M, Kim HM, Beppu T, Miyamoto T, et al. Apatite-forming ability of carboxyl group-containing polymer gels in a simulated body fluid. Biomaterials. 2003;24:2477–84.
9. Kim H-M, Himeno T, Kokubo T, Nakamura T. Process and kinetics of bonelike apatite formation on sintered hydroxyapatite in a simulated body fluid. Biomaterials. 2005;26:4366–73.
10. Lickorish D, Ramshaw JA, Werkmeister JA, Glattauer V, Howlett CR. Collagen-hydroxyapatite composite prepared by biomimetic process. J Biomed Mater Res A. 2004;68A:19–27.
11. You C, Miyazaki T, Ishida E, Ashizuka M, Ohtsuki C, Tanihara M. Fabrication of poly(vinyl alcohol)-apatite hybrids through biomimetic process. J Eur Ceram Soc. 2007;27:1585–8.
12. Kim H-W, Kim H-E, Salih V. Stimulation of osteoblast responses to biomimetic nanocomposites of gelatin-hydroxyapatite for tissue engineering scaffolds. Biomaterials. 2005;26:5221–30.
13. Chen Y, Mak AFT, Wang M, Li J, Wong MS. PLLA scaffolds with biomimetic apatite coating and biomimetic apatite/collagen composite coating to enhance osteoblast-like cells attachment and activity. Surf Coat Technol. 2006;201:575–80.
14. Azevedo HS, Leonor IB, Alves CM, Reis RL. Incorporation of proteins and enzymes at different stages of the preparation of calcium phosphate coatings on a degradable substrate by a biomimetic methodology. Mater Sci Eng C. 2005;25:169–79.
15. Cüneyt Tas A. Synthesis of biomimetic Ca-hydroxyapatite powders at 37°C in synthetic body fluids. Biomaterials. 2000;21:1429–38.
16. Landi E, Tampieri A, Celotti G, Langenati R, Sandri M, Sprio S. Nucleation of biomimetic apatite in synthetic body fluids: dense and porous scaffold development. Biomaterials. 2005;26:2835–45.
17. Kim SS, Park MS, Gwak SJ, Choi CY, Kim BS. Accelerated bonelike apatite growth on porous polymer/ceramic composite scaffolds in vitro. Tissue Eng. 2006;12:2997–3006.
18. Stoch A, Jastrzebski W, Brozek A, Stoch J, Szaraniec J, Trybalska B, et al. FTIR absorption-reflection study of biomimetic growth of phosphates on titanium implants. J Mol Struct. 2000;555:375–82.
19. Müller L, Müller FA. Preparation of SBF with different content and its influence on the composition of biomimetic apatites. Acta Biomater. 2006;2:181–9.
20. Müller L, Conforto E, Caillard D, Müller FA. Biomimetic apatite coatings—carbonate substitution and preferred growth orientation. Biomol Eng. 2007;24:462–6.
21. Oyane A, Kim HM, Furuya T, Kokubo T, Miyazaki T, Nakamura T. Preparation and assessment of revised simulated body fluids. J Biomed Mater Res A. 2003;65A:188–95.
22. Chou Y-F, Huang W, Dunn JCY, Miller TA, Wu BM. The effect of biomimetic apatite structure on osteoblast viability, proliferation, and gene expression. Biomaterials. 2005;26:285–95.
23. Chim H, Hutmacher DW, Chou AM, Oliveira AL, Reis RL, Lim TC, et al. A comparative analysis of scaffold material modifications for load-bearing applications in bone tissue engineering. Int J Oral Maxillofac Surg. 2006;35:928–34.
24. Murphy WL, Hsiong S, Richardson TP, Simmons CA, Mooney DJ. Effects of a bone-like mineral film on phenotype of adult human mesenchymal stem cells in vitro. Biomaterials. 2005;26:303–10.
25. Oyane A, Uchida M, Choong C, Triffitt J, Jones J, Ito A. Simple surface modification of polycaprolactone for apatite deposition from simulated body fluid. Biomaterials. 2005;26:2407–13.
26. Ho M-H, Kuo P-Y, Hsieh H-J, Hsien T-Y, Hou L-T, Lai J-Y, et al. Preparation of porous scaffolds by using freeze-extraction and freeze-gelation methods. Biomaterials. 2004;25:129–38.
27. Hayashi T, Nakayama K, Mochizuki M, Masuda T. Studies on Biodegradable Poly(hexano-6-lactone fibers). Part 3. Enzymatic degradation in vitro. Pure Appl Chem. 2002;74:869–80.
28. Lebourg M, Antón JS, Ribelles JLG. Porous membranes of PLLA-PCL blend for tissue engineering applications. Eur Polym J. 2008;44:2207–18.
29. Adams CS, Mansfield K, Perlot RL, Shapiro IM. Matrix regulation of skeletal cell apoptosis. Role of calcium and phosphate ions. J Biol Chem. 2001;276:20316–22.
30. Chou L, Marek B, Wagner WR. Effects of hydroxylapatite coating crystallinity on biosolubility, cell attachment efficiency and proliferation in vitro. Biomaterials. 1999;20:977–85.
31. Bodhak S, Bose S, Bandyopadhyay A. Role of surface charge and wettability on early stage mineralization and bone cell–materials interactions of polarized hydroxyapatite. Acta Biomater. 2009;5:2178–88.
32. Bohner M, Lemaitre J. Can bioactivity be tested in vitro with SBF solution? Biomaterials. 2009;30:2175–9.
33. Koutsopoulos S. Synthesis and characterization of hydroxyapatite crystals: a review study on the analytical methods. J Biomed Mater Res. 2002;62:600–12.

34. Habibovic P, Sees TM, van den Doel MA, van Blitterswijk CA, de Groot K. Osteoinduction by biomaterials—physicochemical and structural influences. J Biomed Mater Res A. 2006;77A: 747–62.

35. Habibovic P, Yuan H, van der Valk CM, Meijer G, van Blitterswijk CA, de Groot K. 3D microenvironment as essential element for osteoinduction by biomaterials. Biomaterials. 2005; 26:3565–75.